Supportting Information

1. The influence of density on permittivity and permeability of the composite:
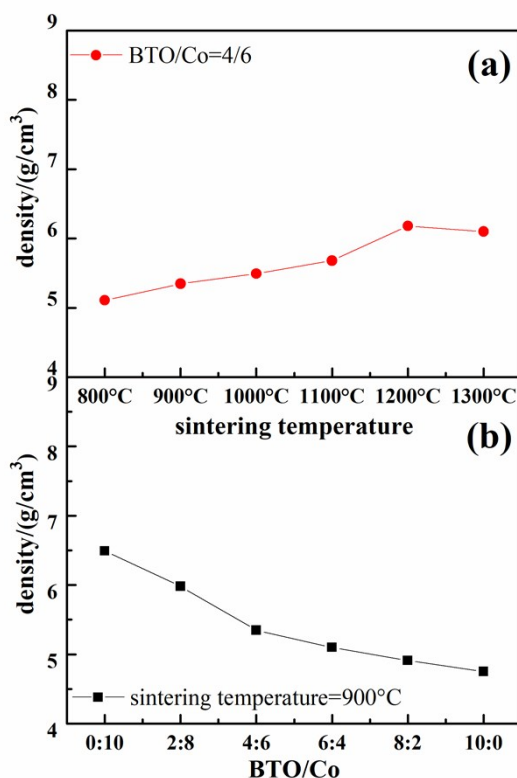

Fig. S1 (a) density of $BaTiO_3/Co_3O_4$ with BTO/Co molar ratio of 4/6 sintered at 800~1300 °C; (b) density of $BaTiO_3/Co_3O_4$ with BTO/Co molar ratio of 0/10~10/0 sintered at 900 °C.

It is shown above in Fig. S1(a) in which the density of the composite increases slowly with the increase in sintering temperature from 800 °C to 1100 °C, having a constant increasing rate of 18.3%. Besides, the density increases sharply with increasing sintering temperature from 1100 °C to 1200 °C and then keeps stable to 1300 °C due to the significantly large grain size obtained. Fig. S1 (b) shows the density of the composite with BTO/Co from 0:10 to 10:0 sintered at constant temperature of 900 °C. It decreases obviously with molar ratio of BTO/Co from low to high. The

decreasing rate of the density with molar fraction of BTO is 28.8% initially from 0 to 4:6 and then is 10% from 4:6 to 10:0. However, in this work, we focus on the samples with molar ratio of BTO/Co of 4:6 and sintered at temperatures from 900 °C to 1100 °C. It is clear from Fig. S1 (a), the density changing a little with sintering temperature is linearly proportional to the increase in grain size. It implies that the influence of density on permittivity and permeability of the powders is based on the influence of grain size. Thus, the grain size as well as the density, will control generation of both permittivity and permeability resonances of the absorption powder at millimeter wave frequency range.

2. The effect of particle size on absorption properties:
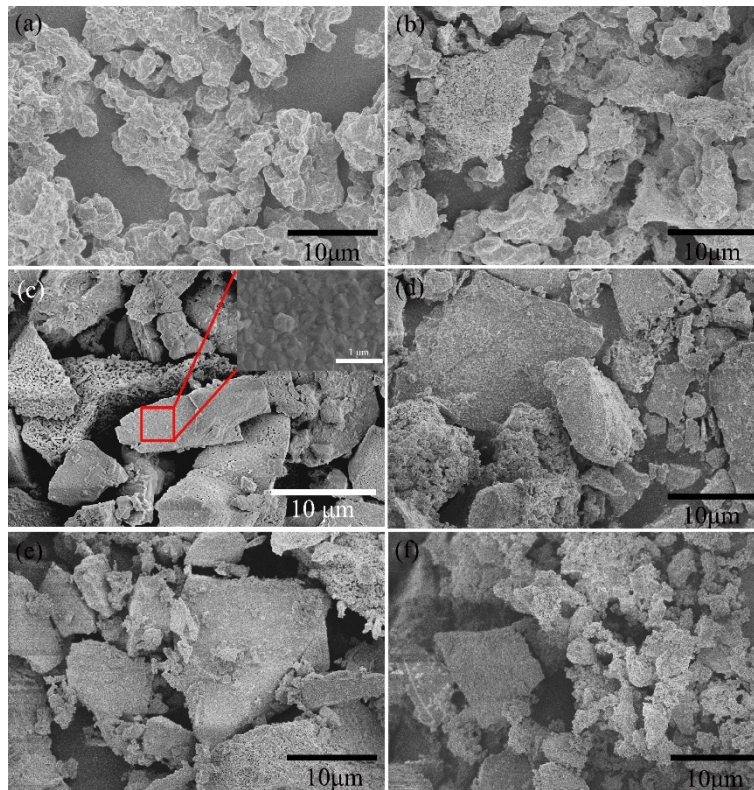

Fig. S2 SEM image of composite powders with BTO/Co of (a)0/10, (b)2/8, (c)4/6, (d)6/4, (e)8/2 and (f)10/0 sintered at 900 °C.
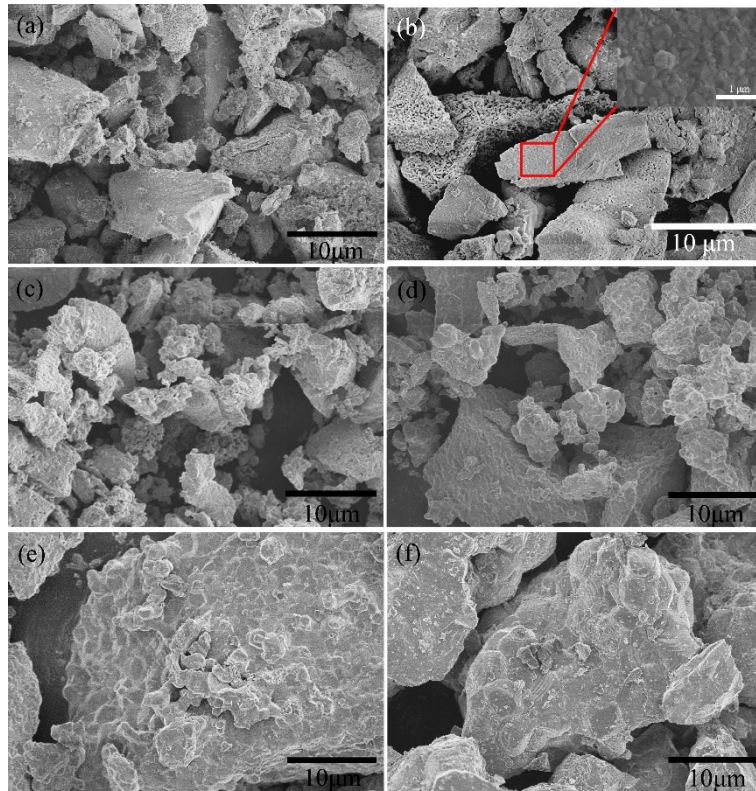
Fig. S3 SEM image of composite powders with BTO/Co of 4/6 sintered at (a)800 °C, (b)900 °C, (c)1000 °C, (d)1100 °C, (e)1200 °C and (f)1300 °C.

Table S1 The particle size (volume percentage v%) of the composite powders with different molar ratio (2/8~8/2) sintered at 900 °C and the 4/6 composite sintered at 800~1300 °C

BTO/Co	Sintering temperature(°C)	Particle size(v%)		
		0~5μm	5~15μm	>15μm
2/8	900	4.2	61.6	35.6
4/6	900	8.8	61.9	29.3
6/4	900	4.8	67.5	27.6
8/2	900	7.2	69.1	23.7
4/6	800	5.9	58.5	35.5
4/6	900	8.8	61.9	29.3
4/6	1000	14.0	52.3	33.7
4/6	1100	5.6	58.0	44.5
4/6	1200	1.5	22.1	76.5
4/6	1300	0.4	19.7	79.9

In Fig. S2, it is seen that as the molar ratio of BTO/Co changes, the particle size, shape and distribution are almost the same one another. All the particle size of samples with different composition ratios are controlled within between 5 and 20 μm and mainly

in about 10 μm. And, the particle size and shape of sample with BTO/Co ratio of 4/6 is not typically different from those of others as well. It implies that the absorption properties of sample with BTO/Co ratio of 4/6 were from intrinsic properties rather than the differences of particle size and shape from others. In addition, the composite powders with BTO/Co ratio of 4/6 sintered below 1100 °C having all 5-15 μm in size as shown in Fig. S3 (a) (b) (c) and (d), and sintered above 1200 °C having the grain size is so large as shown in Fig. S3 (e) (f). Apparently, the former falls in the millimeter frequency range with resonance of permittivity and permeability and the latter are out of the millimeter frequency range.

The detail distribution of the particle size of samples is shown in Table S1. All the particle size of powders with different composition ratios and sintering temperature are mainly between 5 and 15 μm. The distribution of the particle size of the composite sintered below 1100 °C with different molar ratio shows little difference. But the particle size of the 4BTO/6Co composite sintered above 1200 °C is so large, in which most of them are greater than 15 μm.

3． The effect of CoO phase on absorption properties:

In fact, as has been discussed about the formation of CoO phase in the manuscript, the CoO phase forms in some composite sintered above 900 °C. Obviously, as shown in XRD pattern and Table S2, CoO phase begins to form at 900 °C in sample with molar ratio of BTO/Co of 2/8, and at 1000 °C with the molar ratio of 4/6 and 6/4 respectively. And there are no obvious peaks of Co_3O_4 and CoO phases seen in samples with molar ratio of 8/2. Indeed, in the composite, the CoO phase seems to form along with Co_3O_4

phase. The higher the temperature and the higher the content of Co are, the more the CoO phase formed is, as shown in Table S2. For a certain molar ratio of BTO/Co, the content of Co_3O_4 phase decreases with the increase in sintering temperature while increasing content of CoO phase. The formation of CoO phase is dependent on the competition of Co ions between CoO and Co_3O_4 phases. At low temperature, the formation of Co_3O_4 is so strong that Co ions is captured to form Co_3O_4 phase, thus less amount of Co content remained couldn't help to form CoO. Differently, at high temperature, the formation ability of Co_3O_4 is weak. Because of large amount of remaining Co content, CoO is formed easily.

However, in this manuscript, we highlight the synergetic interaction between the two constituent phases of BTO and Co_3O_4 to control the generation of double resonant peaks with appropriate frequency difference over the millimeter wave frequency range, which results in wider bandwidth and strong reflection loss. In such case, the perfect formation of two constituent phases of BTO and Co_3O_4 is in fact important. The existence of CoO may destroy the synergetic interaction between the two phases of BTO and Co_3O_4 and thus the reflection loss and bandwidth weaken to a great extent. As shown in Table S2, the more the content of CoO phase is, the narrower the bandwidth of the composite is. Therefore, only the samples sintered at 900 °C which have mainly the pure constituent phases of BTO and Co_3O_4 formed were discussed in this manuscript. In fact, why the absorption properties of other samples shown as in Fig. 4 decreasing with increasing temperature is due to CoO inside.

Table S2 The bandwidth, peaks' RL and peaks' position (frequency) of the different molar ratio (1/9~8/2) sintered at 800~1300 °C with different content of CoO (weight percentage wt% and volume percentage v%)

BTO/Co	CoO (wt%)	CoO (v%)	Sintering temperature (°C)	Bandwidth (GHz)	BTO/Co	CoO (wt%)	CoO (v%)	Sintering temperature (°C)	Bandwidth (GHz)
1/9	0	0	800	3.4	5/5	0	0	800	4.2
1/9	7	6.6	900	2.6	5/5	0	0	900	3.1
1/9	9.5	9.0	1000	2.8	5/5	6.2	5.8	1000	2.2
1/9	12.6	11.9	1100	1.9	5/5	5.6	5.3	1100	2.7
1/9	13.9	13.2	1200	0	5/5	6.1	5.7	1200	2
1/9	21.3	20.2	1300	0	5/5	16.9	16.0	1300	1.3
2/8	0	0	800	4.7	6/4	0	0	800	2.6
2/8	4.3	4.0	900	3.2	6/4	0	0	900	2.9
2/8	6.3	5.9	1000	3	6/4	3.4	3.2	1000	2.1
2/8	8.6	8.1	1100	2.8	6/4	3.9	3.7	1100	1.8
2/8	12.0	11.3	1200	2.6	6/4	6.7	6.3	1200	1.3
2/8	19.1	18.1	1300	1	6/4	9.8	9.2	1300	2.1
3/7	0	0	800	4.7	7/3	0	0	800	3.3
3/7	3.3	3.1	900	3.1	7/3	0	0	900	3.5
3/7	9.3	8.8	1000	2.6	7/3	4.6	4.3	1000	2.1
3/7	7.2	6.8	1100	2.3	7/3	5.2	4.9	1100	2.1
3/7	10.3	9.7	1200	2.5	7/3	10.1	9.5	1200	1.7
3/7	14.4	13.6	1300	0.4	7/3	12.5	11.8	1300	1.7
4/6	0	0	800	4	8/2	0	0	800	3.4
4/6	0	0	900	5	8/2	0	0	900	3.6
4/6	4.5	4.2	1000	4	8/2	0	0	1000	4.9
4/6	5.4	5.1	1100	4.5	8/2	0	0	1100	3.7
4/6	10.4	9.8	1200	4	8/2	0	0	1200	2.3
4/6	13.7	12.9	1300	2.2	8/2	0	0	1300	3.3

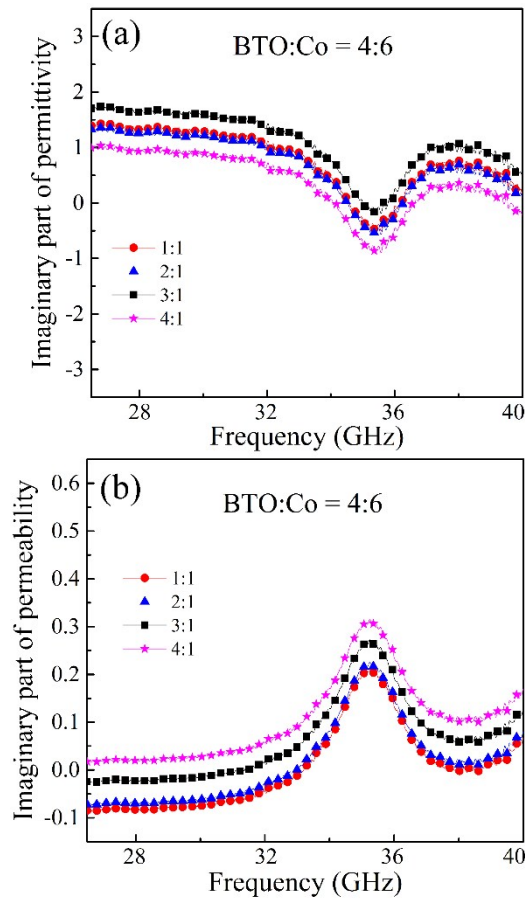## 4. The effect of different mass ratio with paraffin:

Fig. S4 The imaginary part of permittivity (a) and permeability (b) of the composite with BTO/Co 4/6 sintered at 900 °C, with different weight ratio of the sample and paraffin (1:1, 2:1, 3:1, and 4:1).

The Fig. S4 (a) (b) shows the electromagnetic factors of imaginary part of permittivity (ε'') and permeability (μ'') of the samples with paraffin with different weight ratio of 1:1, 2:1, 3:1 and 4:1. It is seen that all the samples with different weight ratios behave almost the same aspects of ε'' and μ'' with frequency. We know that the paraffin serves as a "shaping agent" without interaction with EM wave in general to make the composite powders form "soft solid" state into rectangular slots of copper molds for measurement of electromagnetic parameters. The paraffin actually affects weakly aspects of the composite powders changing with frequency although the intensity of electromagnetic wave absorption changes a little due to the content change

of the powders in the mixed system. As shown in references[1-6], the electromagnetic properties of the samples with different ratio of paraffin over powder content in the mixed system keep almost the same aspects of dielectric and magnetic properties. Due to that the transmittal line theory is used, the aspects of absorption properties of the samples will keep almost same although depending on an appropriate matching factor. Thus, the weight ratio of 4:1 which is traditionally applied by many researchers in area of measurement of absorption properties was used.

5. The influence of $|Z_{in}|$ with different molar ratios on absorption properties:

To guarantee the effective EM wave absorption, it is inclined to decline the both of reflected EM waves and increase absorption ability of EM wave. Chief of all, the highly effective injection of EM wave from surface into the absorber is importantly controlled by making Z_{in} close to Z_0 ($|Z_{in}|=Z_{in}/Z_0$, close to 1), which is called impedance matching, to make RL approach more negative (high reflection loss). As shown in Fig. S5, $|Z_{in}|$ of composites with different molar ratios is provided. The composites of molar ratio 4/6 sintered at 900 ℃ possess that $|Z_{in}|$ is close to 1. Besides, the two frequencies (about 35 GHz, 37 GHz) where $|Z_{in}|$ is most close to 1 correspond the two frequencies of the strongest RL, which further supports the opinions above.
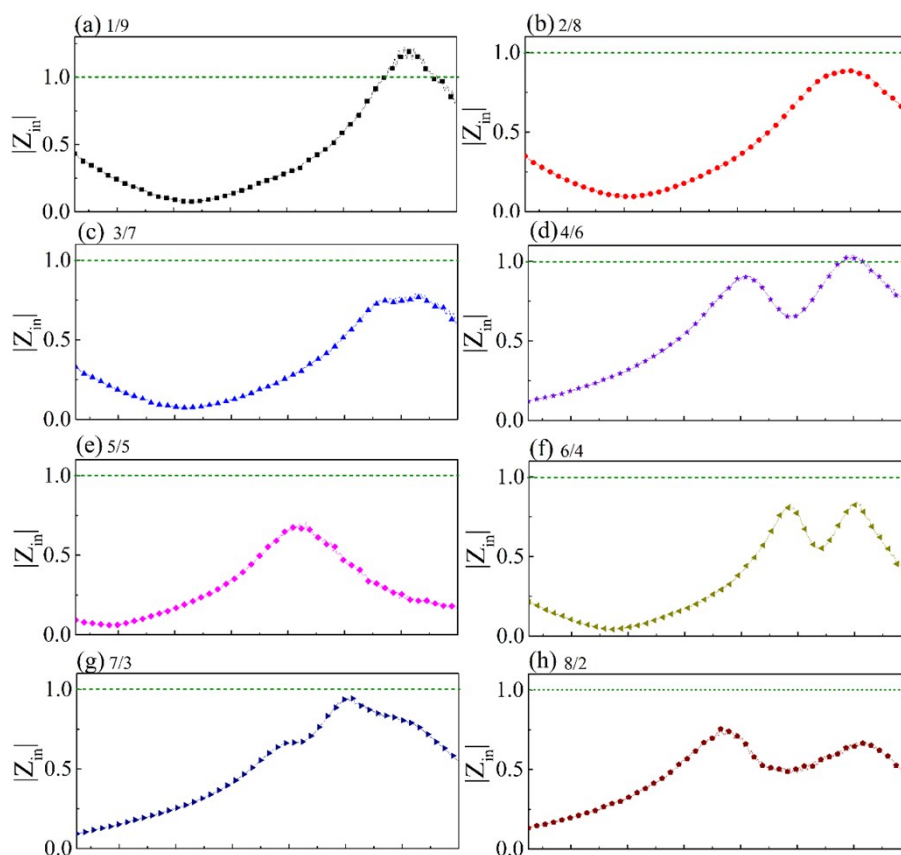
Fig. S5 the $|Z_{in}|$ ($|Z_{in}|= Z_{in}/Z_0$) of BTO/Co$_3$O$_4$ sintered at 900 °C with different molar ratios: (a)1/9, (b)2/8, (c)3/7, (d)4/6, (e)5/5, (f)6/4, (g)7/3 and (h)8/2.

Reference

1. Z. Liu, J. Yuan, K. Li, Xiong, Kuangwei, S. Jin and P. Wang, *J. Electron. Mater.*, 2018, **47**, 4910-4918.

2. C. Y. Liu, Y. J. Chen, Y. Y. Yue, Y. Tang, Z. R. Wang, N. Ma and P. Y. Du, *J. Am. Ceram. Soc.*, 2017, **100**, 3999-4010.

3. C. Y. Liu, Y. J. Zhang, Y. Tang, Z. R. Wang, H. C. Tang, Y. Ou, L. Yu, N. Ma and P. Y. Du, *Phys. Chem. Chem. Phys.*, 2017, **19**, 21893-21903.

4. C. Y. Liu, Y. J. Zhang, Y. Tang, Z. R. Wang, N. Ma and P. Y. Du, *J. Mater. Chem. C*, 2017, **5**, 3461-3472.

5. C. Y. Liu, Q. K. Xu, Y. Tang, Z. R. Wang, R. Y. Ma, N. Ma and P. Y. Du, *J. Mater. Chem. C*, 2016, **4**, 9532-9543.

6. Y. Lin, J. Dai, H. Yang, L. Wang and F. Wang, *Chem. Eng. J.*, 2018, **334**, 1740-1748.